Aryl-Perfluoroaryl Interaction in Two-Dimensional Organic–Inorganic Hybrid Perovskites Boosts Stability and Photovoltaic Efficiency

Jun Hu,[†] Iain W. H. Oswald,[‡] Huamin Hu,[†] Samuel J. Stuard,[§] Masrur Morshed Nahid,[§] Liang Yan,[†] Zheng Chen,[†] Harald Ade,[§] James R. Neilson,[‡] and Wei You*[,†,∥]

[†]Department of Chemistry, University of North Carolina at Chapel Hill, Chapel Hill, North Carolina 27599, United States

[‡]Department of Chemistry, Colorado State University, Fort Collins, Colorado 80523, United States

[§]Department of Physics, North Carolina State University, Raleigh, North Carolina 27695, United States

[∥]Department of Applied Physical Sciences, University of North Carolina at Chapel Hill, Chapel Hill, North Carolina 27599, United States

ABSTRACT: **Two-dimensional (2D) organic–inorganic hybrid perovskites (OIHPs) have showed impressive stability, compared to their three-dimensional (3D) counterparts. However, tuning the chemical structure of the organic cations to simultaneously improve the device performance and stability of 2D OIHP solar cells is rarely reported. Here, we demonstrate that by introducing a classic noncovalent aryl-perfluoroaryl interaction, 2D OIHP solar cells with 1:1 mixed phenethylammonium (PEA) and perfluorophenethylammonium (F5-PEA) can achieve an efficiency of >10% with much enhanced stability using a simple deposition at low temperature without using any additives. The competing effects of surface morphology and crystal orientation with an increased amount of F5-PEA result in the highest efficiency at a 1:1 ratio, while single-crystal studies reveal the expected aryl-perfluoroaryl interaction, accounting for the highest device stability of 2D OIHP solar cell at 1:1 ratio as well. This work provides an example where tuning the interactions of organic cations via molecular engineering can have a profound effect on device performance and stability of 2D OIHP solar cells.**

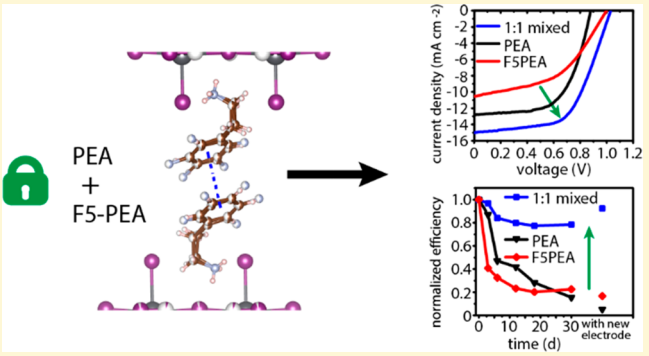

Organic–inorganic hybrid perovskites (OIHPs)-based solar cells have observed tremendous improvement in power conversion efficiency up to 20%.[1−10] However, typical OIHP materials for high-efficiency devices are not stable under ambient conditions.[11−20] Recently, reducing the dimension of the materials from three-dimensional (3D) OIHPs to two-dimensional (2D) (or quasi-2D, layered) materials has been shown as an effective way to improve the stability of OIHP solar cells.[21−25] These 2D OIHPs have a general formula of $(RNH_3)_2MA_{n-1}Pb_nI_{3n+1}$, in which n represents the number of lead iodide octahedra between adjacent insulating organic cation layers (RNH_3^+).[26,27] Different from their 3D counterpart, which would have reactive dangling bonds or amorphous species in grain boundaries,[17] these layered 2D OIHPs can be viewed as "3D" OIHPs slabs being passivated with organic cations. This passivation could be one of the main reasons for the enhanced stability of such OIHPs.[21−23,28]

Recently, 2D OIHPs solar cells have been demonstrated to have significant high efficiency via a couple of methods, such as hot-casting[29] and additives;[30−34] the stability of 2D OIHPs has also been shown to be greatly improved (when compared with 3D counterparts).[29−35] For example, by applying methylammonium chloride as the additive, 2D OIHP based on 3-bromobenzylammonium iodide can achieve an efficiency of 18.20% and maintain 82% of their initial efficiency after 2400 h under a relative humidity (RH) of ∼40%.[34] By applying the same additive, 2D OIHP based on 2-thiophenemethylammonium achieved an efficiency of >15% with 90% of its initial efficiency after a storage time of 1000 h.[33]

Received: April 8, 2019
Accepted: June 5, 2019
Published: June 5, 2019

DOI: 10.1021/acsmaterialslett.9b00102
ACS Materials Lett. 2019, 1, 171−176

Most 2D OIHPs for solar cells employ large organic cations containing one ammonium ($-NH_3^+$) group anchored into the inorganic framework and one organic chain extending out from it. Typically, two layers of such spacers, via van der Waals interactions, form the organic insulating layer that separates the inorganic layers. These van der Waals interactions are nonspecific, nondirectional, and highly distance dependent, which are not ideal to stabilize the enclosed OIHPs. Applying spacer cations with diammoniums (NH_3^+-R-NH_3^+) can eliminate the van der Waals interactions and apply covalent bonding instead to link inorganic layers, which, in principle, should offer much improved stability. Indeed, diammoniums have recently been adopted into 2D OIHPs (i.e., Dion-Jacobsen phase 2D OIHPs) to achieve a higher device stability.[36−40] However, most of the works with diammoniums require relatively harsh processing conditions, such as hydroiodic acid as the additive[37] or long-time and/or high-temperature annealing[38−40] to achieve typical diffraction and absorption behavior of 2D OIHPs. It appears that the 2D OIHP films with diammonium cations are much harder to form, likely because of the poor defect tolerance (e.g., requiring the positioning of the *two* ammoniums of *one* spacer cation onto *two* adjacent inorganic layers simultaneously).

To overcome these issues with conventional monoammonium and diammonium cations, we envisioned a *strong noncovalent* interaction between the organic chains of monoammonium cations (R-NH_3^+). This would still allow a facile formation of 2D OIHPs because of monoammonium cations, yet with much improved stability via the strong noncovalent interaction between these organic chains. Here, we show that the well-known quadrupole−quadrupole interaction between perfluorobenzene and benzene can be used to achieve much improved device stability (maintaining 92% of the original efficiency after 30 days without encapsulation) of 2D OIHPs solar cells with appreciable efficiency values (~11%). In addition, our film deposition was very simple, only requiring a quick annealing at low temperature (40 °C for 30 s) after casting the precursor solution.

The aryl-perfluoroaryl interaction is a widely studied noncovalent interaction, which, for example, can solidify an equimolar of benzene and hexafluorobenzene in an alternating manner at 23.7 °C.[41] This strong interaction has been widely used in supramolecular and polymer chemistries.[41−46] In our study, we chose phenethylammonium ($C_6H_5-CH_2CH_2-NH_3^+$, PEA) and 2,3,4,5,6-pentafluorophenethylammonium ($C_6F_5-CH_2CH_2-NH_3^+$, F5-PEA) as the spacer cations to introduce the aryl-perfluoroaryl interaction into 2D OIHPs.

Experimentally, 2D OIHP with stoichiometric n = 4 (see Figures 1a and 1b) was chosen as the active layer in a *p*-i-*n* planar structured solar cell.[47] As shown in Figure 1c, as well as Table S1 and Figure S2 in the Supporting Information, we achieved an efficiency of 7.64% with a small hysteresis for device with PEA only, which is comparable to the reported efficiency (for a small n value) without additives or hot-casting.[22,23,48,49] Interestingly, substituting 25 mol % of the PEA with an equivalent amount of F5-PEA led to an increase in both open-circuit voltage (V_{oc}) and short-circuit current (J_{sc}) of the solar cell. Raising the amount of F5-PEA to 50 mol % further improved the device characteristics and reached an efficiency value of 10.24%. However, further increases in the amount of F5-PEA (i.e., 75% and 100%) resulted in lower device performance and more serious hysteresis (see Figure S2a in the Supporting Information). Furthermore, the 50% F5-PEA (i.e., PEA:F5-PEA = 1:1)-based solar cells

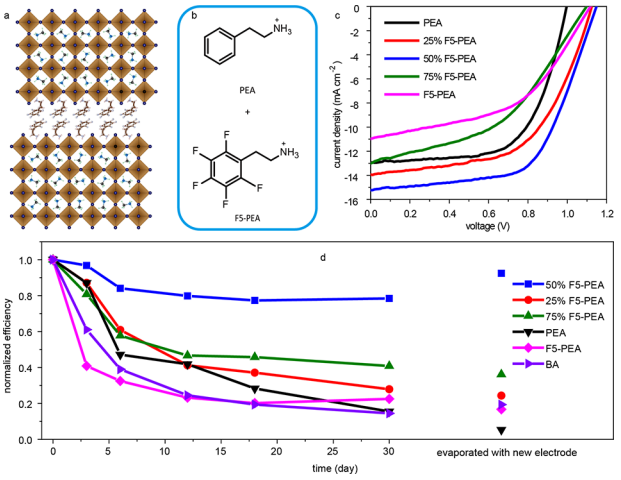

Figure 1. 2D OIHPs and characterization of their photovoltaic devices: (a) crystal sketch of PEA/F5-PEA 2D OIHP (n = 4); (b) molecular structures of PEA and F5-PEA; (c) current-density−voltage (J−V) curves (forward scan) under 1 sun condition (AM 1.5G); (d) stability of unencapsulated 2D OIHP solar cells for 30 days under 45% relative humidity. The last data point represents the same device after 30 days but with a newly evaporated electrode.

demonstrated the best stability among this series of solar cells tested (including the well-studied butylammonium (BA)-based 2D OIHPs), maintaining more than 80% of its original efficiency after 30 days under ambient condition (RH = 45%; see Figure 1d). In addition, depositing fresh electrodes on the same devices after 30 days could recover 92% of the initial efficiency. This observation indicates that the damage of the metal electrode such as mechanical scratching or oxidation during testing could be the main reason for the performance degradation of the 50% F5-PEA-based devices. In contrast, we did not observe similar efficiency recovery for other 2D OIHPs-based solar cells. We further tested the stability under continuous illumination at working condition (unencapsulated, RH = 55%; see Figure S3 in the Supporting Information) and a similar trend was observed. These results clearly demonstrate that 50% F5-PEA 2D OIHP-based solar cells are *intrinsically* much more stable than all other solar cells in our study.

To understand the performance and stability difference of 2D OIHP solar cells with various amounts of F5-PEA, we first applied ultraviolet−visible light (UV-Vis) and photoluminescence (PL) measurements to probe the composition of these 2D OIHP films. Both UV-Vis spectra (Figure 2a) and PL spectra with excitation from the glass substrate side (Figure 2b) clearly indicate the presence of multiple 2D OIHP phases (e.g., n = 1, 2, 3, etc.) in all films. The UV-Vis spectra (Figure 2a) also suggest a similar amount of each phase in different films. Therefore, the light-absorbing capability is not the main reason for the observed different device efficiency. In addition, the absorption and emission peaks of each 2D phase are narrow and do not show peak splitting, indicating that the mixed F5-PEA- and PEA-based 2D OIHP films are *not* a mixture of spatially separated F5-PEA-based and PEA-based 2D OIHP domains. Further study of 2D OIHP films with the n = 1 phase only (Figures S7 and S8 in the Supporting Information) also supported our observation that these F5-PEA and PEA cations in the OIHP structure form a solid solution in the interlayer gallery, which will be further discussed by the single-crystal structure (vide infra). In addition, the PL spectra with excitation from the air side exhibit much weaker intensities of 2D OIHP peaks, compared to that of 3D

DOI: 10.1021/acsmaterialslett.9b00102
ACS Materials Lett. 2019, 1, 171−176

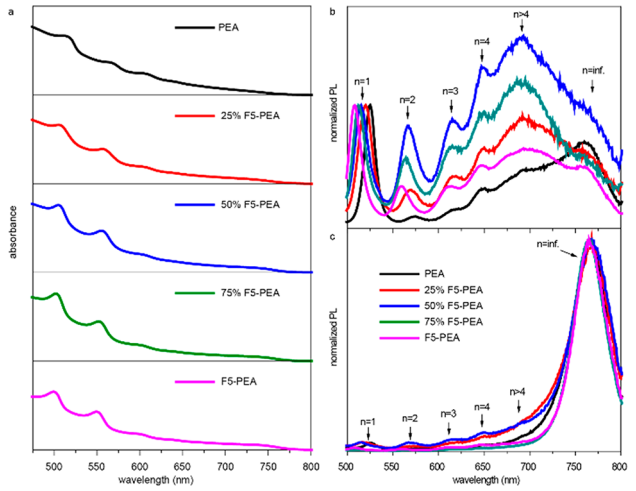

Figure 2. Optical properties of 2D OIHP films: (a) UV-Vis absorption; (b) PL from the substrate side (normalized to the n = 1 peak), and (c) PL from the air side (normalized to the n = inf. peak). Numbers and arrows indicate signals from different phases.

(Figure 2c), indicating a vertical phase segregation of different n numbers as we and other researchers observed previously, which is beneficial (or even crucial) to achieving efficient 2D OIHP solar cells.[47,50,51]

We next investigated the surface morphology of our 2D OIHP. Shown in Figure 3a, 2D OIHP film with PEA as the sole

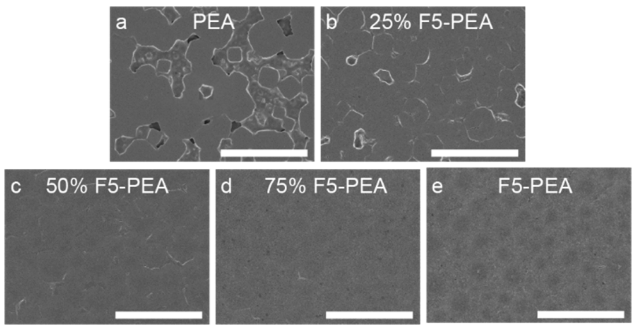

Figure 3. Surface morphology of 2D OIHP films: SEM images of 2D OIHP films with (a) 0%, (b) 25%, (c) 50%, (d) 75%, and (e) 100% F5-PEA. Scale bar = 5 μm.

spacer cation has many visible pinholes from the scanning electron microscopy (SEM) image. These pinholes became much smaller in the film having 25% F5-PEA (Figure 3b) and finally disappeared with 50% F5-PEA or more (see Figures 3c–e). A similar evolution of the surface morphology was also observed with atomic force microscopy (AFM) (see Figure S4 in the Supporting Information). It can also be clearly visualized that the films containing 50% F5-PEA or more show large domains up to several micrometers in size (see Figures S4a–S4j) and the phase image indicates that the domains have uniform composition (see Figures S4k–S4o). The pinholes in the films containing a low amount of F5-PEA (i.e., 0% and 25%) cause nonideal interfacial contact between different layers in the device, which would account for the relatively low device performance (especially V_{oc}). We believe the lower solubility of F5-PEA could lead to a quicker formation of the 2D OIHPs under annealing, which could finally give rise to a more compact film surface morphology. However, even with a pin-hole-free surface morphology, the films having a large amount of F5-PEA (i.e., 75% and 100%) still observed decrease in J_{sc} and fill factor (FF) in the solar cells. Thus, there must be other factors causing the poor performance of 2D OIHP solar cells with a large amount of F5-PEA, such as crystal orientation.

To gain insights on the crystal orientation in our 2D OIHP films, we employed grazing-incidence wide-angle X-ray scattering (GIWAXS).[52] Shown in Figure 4a, the 2D OIHP

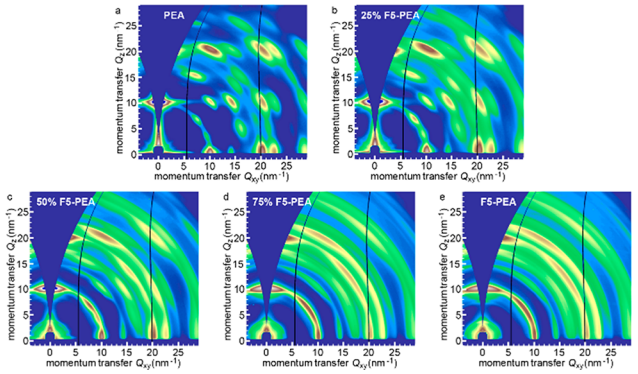

Figure 4. GIWAXS patterns of 2D OIHP films with different amounts of F5-PEA: (a) 0% F5-PEA, (b) 25% F5-PEA, (c) 50% F5-PEA, (d) 75% F5-PEA, and (e) 100% F5-PEA.

film based on PEA shows diffraction spots, indicating a highly orientated film.[29] With more F5-PEA (see Figures 4b–e), diffraction rings start to appear and eventually dominate the diffraction patterns in the case of 75% or 100% F5-PEA-based 2D OIHP film. This random crystal orientation can lead to decreased J_{sc} and FF values, because of the poor transport, which is consistent with the J–V curve. This gradual change in GIWAXS patterns indicates that, with more F5-PEA, the crystallites in the 2D OIHP film start to adopt a more random orientation and texture. As reported by others, the random orientation of 2D OIHP films can be caused by the quick formation of the crystallites,[53,54] which again agrees with our observation of the film surface morphology. However, crystallite orientation is not the only performance-affecting feature that changes with addition of F5-PEA. As shown above, SEM shows *better* surface coverage as the F5-PEA content increases, which should help the device performance. Overall, the competing effects of surface morphology and crystal orientation lead to the best device performance at a PEA:F5-PEA ratio of 1:1.

While all the preceding results explain why 1:1 PEA:F5-PEA-based 2D OIHP solar cells offered the highest efficiency, they only minimally address why 1:1 PEA:F5-PEA-based solar cells also demonstrated the highest stability. First of all, we do not believe that the hydrophobic nature of fluorinated PEA or the improved film quality—shown to be contributing factors to the moisture stability of 2D OIHP in other reported studies[17,55]—is the major reason for the improved stability in our study. This is because we did not observe significantly improved stability of 2D OIHP solar cells as the amount of F5-PEA increases (Figure 1d); instead, the significantly improved stability *only* appears at a PEA:F5-PEA ratio of 1:1.

Given the strong quadrupole–quadrupole interaction in the aryl-perfluoroaryl system,[41−46] we hypothesized that PEA and F5-PEA would form a 1:1 pair via the strong quadrupole–quadrupole interaction to "lock in" the interface of 2D/3D OIHP phases and stabilize the OIHP-film-based devices. To experimentally verify this hypothesis, we grew single crystals of

DOI: 10.1021/acsmaterialslett.9b00102
ACS Materials Lett. 2019, 1, 171–176

the mixed cations based 2D OIHP with $n = 1$ (i.e., $((PEA)_{0.5}(F5\text{-}PEA)_{0.5})_2PbI_4$), since the $n = 1$ phase is the simplest representation of the interface between different 2D/3D OIHP phases. The differences of cation packing are highlighted in Figure 5. The crystal structure of $((PEA)_{0.5}(F5\text{-}PEA)_{0.5})_2PbI_4$

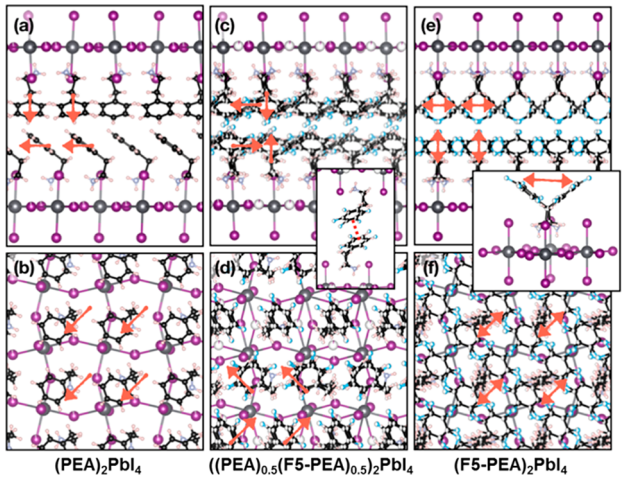

Figure 5. Single-crystal structures of 2D OIHPs: (a, b) $(PEA)_2PbI_4$, showing the collinear packing of PEA molecules (this structure was redrawn based on the work reported by Du et al.[60]), and (c, d) $((PEA)_{0.5}(F5\text{-}PEA)_{0.5})_2PbI_4$, showing the herringbone packing of the organic molecules, which are randomly substituted on the same site. The inset highlights the offset face-to-face packing of a pair of organic cations. (e, f) $(F5\text{-}PEA)_2PbI_4$, showing the collinear packing of 5F-PEA, which does not permit face-to-face interactions. The inset shows the equally occupied and disordered orientations of 5F-PEA; occupancy of either orientation leads to a collinear packing of the molecules, which does not permit face-to-face interactions. Arrows denote the vector of the $^+NH_3CH_2CH_2$−aryl bond.

is disordered, wherein the two different cations lay on top of each other (see Figures 5c and 5d), which is a feature that has been reported in 2D OIHPs with similar aryl-perfluoroaryl interaction.[56,57] Importantly, the herringbone packing in 2D OIHP (Figure 5d) permits two cations to interact in an offset face-to-face or partially eclipsed manner (see the inset in Figure 5d).[56,58,59] While the crystallography does not permit us to explicitly observe interactions between the PEA and F5-PEA, because of their random mixing within the structure, this face-to-face packing motif was *not* observed in 2D OIHP based on PEA alone or F5-PEA alone, as seen in $(PEA)_2PbI_4$[60] and $(F5\text{-}PEA)_2PbI_4$ (see Figures 5a and 5b and Figures 5e and 5f, even in the presence of disorder), highlighting the pivotal role of the quadrupole−quadrupole interaction to create this co-facial packing motif.

To further probe the effect of the aryl-perfluoroaryl interaction on stability, we conducted differential scanning calorimetry (DSC) measurements on the three single crystals. Similar to what was reported by Li et al.,[61] for all three single crystals, we observed two transition peaks, which could be assigned to structure transition (lower temperature) and melting (higher temperature) (see Figure S11 in the Supporting Information). The structure transition enthalpy of the 1:1 PEA:F5-PEA-based 2D OIHP is significantly higher than those of single-cation-based ones. This result further supports that the strong aryl-perfluoroaryl interaction could be the main reason for the improved stability of 1:1 PEA:F5-PEA-based 2D OIHP solar cells.

In summary, we find that introducing a perfluorinated phenethylammonium, F5-PEA, into the PEA-based 2D OIHP can improve the efficiency of such 2D OIHP-based solar cells with significantly improved stability. The incorporation of F5-PEA appears to have competing effects on surface morphology and crystal orientation as the amount of F5-PEA increases, resulting in the highest solar cell efficiency at a 1:1 ratio (50% F5-PEA) with PCE > 10%. More importantly, the highest stability of 1:1 PEA:F5-PEA-based 2D OIHP solar cells can be ascribed to the aryl-perfluoroaryl interaction, which is a strong noncovalent interaction that not only improves the structure stability of the 2D OIHP reported in this study but also largely explains their impressive device stability.

Our study offers a compelling example where a strong noncovalent interaction can significantly affect the structure of 2D OIHPs and the texture of their films and, as a result, boost the efficiency and stability of the solar cells. Given the large body of work in applying various noncovalent interactions in organic, supramolecular, and polymer chemistry,[62−64] we believe that further exploration of these rich chemistries via creative design of new functional cations to incorporate within the 2D OIHPs would achieve desirable device characteristics, as well as industry-standard stability.

■ ASSOCIATED CONTENT

Supporting Information

The Supporting Information is available free of charge on the ACS Publications website at DOI: 10.1021/acsmaterialslett.9b00102.

X-ray crystallographic data for $(F5\text{-}PEA)_2PbI_4$ (CIF)
X-ray crystallographic data for $((PEA)_{0.5}(F5\text{-}PEA)_{0.5})_2PbI_4$ (CIF)
Materials, experimental procedures of SEM, AFM, GIWAXS, single-crystal X-ray diffraction, $J-V$ curves with different scan directions and DSC (PDF)

■ AUTHOR INFORMATION

Corresponding Author

*E-mail: wyou@unc.edu.

ORCID

Jun Hu: 0000-0002-6997-0174
Liang Yan: 0000-0003-4122-7466
James R. Neilson: 0000-0001-9282-5752
Wei You: 0000-0003-0354-1948

Author Contributions

The manuscript was written through contributions of all authors.

Notes

The authors declare no competing financial interest.

■ ACKNOWLEDGMENTS

J.H., L.Y., and W.Y. are supported by the National Science Foundation (No. DMR-1728921) and UNC Research Opportunities Initiative (ROI) through the Center of Hybrid Materials Enabled Electronic Technology. This ROI grant also supports M.M.N. and H.A. Research of solar cell stability test and film morphology was supported by the Center for Hybrid Organic Inorganic Semiconductors for Energy (CHOISE), an Energy Frontier Research Center funded by the U.S. Department of Energy (DOE), Office of Science, Office of Basic Energy Sciences (BES). The SEM and AFM in this work was performed

in part at the Chapel Hill Analytical and Nanofabrication Laboratory (CHANL), a member of the North Carolina Research Triangle Nanotechnology Network (RTNN), which is supported by the National Science Foundation (Grant No. ECCS-1542015), as part of the National Nanotechnology Coordinated Infrastructure (NNCI). J.H. and W.Y. thank Sara Wehlin and Professor Gerald Meyer (UNC−Chapel Hill) for assistance with PL measurements. S.J.S. is supported by the National Science Foundation, under Grant No. DGE-1633587. The GIWAXS measurements were performed at beamline 7.3.3 at the ALS at LBNL, which is supported by the U.S. Department of Energy Grant No. DE-AC02-05CH11231. Experimental support for GIWAXS was provided by C. Zhu and A. Liebman-Pelaez. Work at Colorado State University was supported by Grant No. DE-SC0016083, funded by the U.S. Department of Energy, Office of Science. J.R.N. acknowledges support from Research Corporation for Science Advancement through a Cottrell Scholar Award and the A.P. Sloan Foundation for a Sloan Research Fellowship.

REFERENCES

(1) Kojima, A.; Teshima, K.; Shirai, Y.; Miyasaka, T. Organometal Halide Perovskites as Visible-Light Sensitizers for Photovoltaic Cells. *J. Am. Chem. Soc.* **2009**, *131*, 6050−6051.

(2) Lee, M. M.; Teuscher, J.; Miyasaka, T.; Murakami, T. N.; Snaith, H. J. Efficient Hybrid Solar Cells Based on Meso-Superstructured Organometal Halide Perovskites. *Science* **2012**, *338*, 643−647.

(3) Shin, S. S.; Yeom, E. J.; Yang, W. S.; Hur, S.; Kim, M. G.; Im, J.; Seo, J.; Noh, J. H.; Seok, S. I. Colloidally prepared La-doped $BaSnO_3$ electrodes for efficient, photostable perovskite solar cells. *Science* **2017**, *356*, 167−171.

(4) Jiang, Q.; Zhang, L.; Wang, H.; Yang, X.; Meng, J.; Liu, H.; Yin, Z.; Wu, J.; Zhang, X.; You, J. Enhanced electron extraction using SnO_2 for high-efficiency planar-structure $HC(NH_2)_2PbI_3$-based perovskite solar cells. *Nat. Energy* **2017**, *2*, 16177.

(5) Saliba, M.; Matsui, T.; Domanski, K.; Seo, J.-Y.; Ummadisingu, A.; Zakeeruddin, S. M.; Correa-Baena, J.-P.; Tress, W. R.; Abate, A.; Hagfeldt, A.; Grätzel, M. Incorporation of Rubidium Cations into Perovskite Solar Cells Improves Photovoltaic Performance. *Science* **2016**, *354*, 206−209.

(6) Yang, W. S.; Park, B.-W.; Jung, E. H.; Jeon, N. J.; Kim, Y. C.; Lee, D. U.; Shin, S. S.; Seo, J.; Kim, E. K.; Noh, J. H.; Seok, S. I. Iodide Management in Formamidinium-Lead-Halide−Based Perovskite Layers for Efficient Solar Cells. *Science* **2017**, *356*, 1376−1379.

(7) Huang, J.; Yuan, Y.; Shao, Y.; Yan, Y. Understanding the Physical Properties of Hybrid Perovskites for Photovoltaic Applications. *Nat. Rev. Mater.* **2017**, *2*, 17042.

(8) Jeon, N. J.; Na, H.; Jung, E. H.; Yang, T.-Y.; Lee, Y. G.; Kim, G.; Shin, H.-W.; Il Seok, S.; Lee, J.; Seo, J. A Fluorene-Terminated Hole-Transporting Material for Highly Efficient and Stable Perovskite Solar Cells. *Nat. Energy* **2018**, *3*, 682−689.

(9) Zuo, C.; Vak, D.; Angmo, D.; Ding, L.; Gao, M. One-Step Roll-To-Roll Air Processed High Efficiency Perovskite Solar Cells. *Nano Energy* **2018**, *46*, 185−192.

(10) Fang, Z.; Liu, L.; Zhang, Z.; Yang, S.; Liu, F.; Liu, M.; Ding, L. $CsPbI_{2.25}Br_{0.75}$ Solar Cells with 15.9% Efficiency. *Science Bulletin* **2019**, *64*, 507−510.

(11) Rong, Y.; Hu, Y.; Mei, A.; Tan, H.; Saidaminov, M. I.; Seok, S. I.; McGehee, M. D.; Sargent, E. H.; Han, H. Challenges for Commercializing Perovskite Solar Cells. *Science* **2018**, *361*, eaat8235.

(12) Baikie, T.; Fang, Y.; Kadro, J. M.; Schreyer, M.; Wei, F.; Mhaisalkar, S. G.; Graetzel, M.; White, T. J. Synthesis and Crystal Chemistry of the Hybrid Perovskite $(CH_3NH_3)PbI_3$ for Solid-State Sensitised Solar Cell Applications. *J. Mater. Chem. A* **2013**, *1*, 5628−5641.

(13) Niu, G.; Guo, X.; Wang, L. Review of Recent Progress in Chemical Stability of Perovskite Solar Cells. *J. Mater. Chem. A* **2015**, *3*, 8970−8980.

(14) Stoumpos, C. C.; Malliakas, C. D.; Kanatzidis, M. G. Semiconducting Tin and Lead Iodide Perovskites with Organic Cations: Phase Transitions, High Mobilities, and Near-Infrared Photoluminescent Properties. *Inorg. Chem.* **2013**, *52*, 9019−9038.

(15) Wang, Q.; Dong, Q.; Li, T.; Gruverman, A.; Huang, J. Thin Insulating Tunneling Contacts for Efficient and Water-Resistant Perovskite Solar Cells. *Adv. Mater.* **2016**, *28*, 6734−6739.

(16) Cheacharoen, R.; Rolston, N.; Harwood, D.; Bush, K. A.; Dauskardt, R. H.; McGehee, M. D. Design and Understanding of Encapsulated Perovskite Solar Cells to Withstand Temperature Cycling. *Energy Environ. Sci.* **2018**, *11*, 144−150.

(17) Wang, Q.; Chen, B.; Liu, Y.; Deng, Y.; Bai, Y.; Dong, Q.; Huang, J. Scaling Behavior of Moisture-Induced Grain Degradation in Polycrystalline Hybrid Perovskite Thin Films. *Energy Environ. Sci.* **2017**, *10*, 516−522.

(18) Li, X.; Ibrahim Dar, M.; Yi, C.; Luo, J.; Tschumi, M.; Zakeeruddin, S. M.; Nazeeruddin, M. K.; Han, H.; Grätzel, M. Improved Performance and Stability of Perovskite Solar Cells by Crystal Crosslinking with Alkylphosphonic Acid ω-Ammonium Chlorides. *Nat. Chem.* **2015**, *7*, 703.

(19) Yang, S.; Wang, Y.; Liu, P.; Cheng, Y.-B.; Zhao, H. J.; Yang, H. G. Functionalization of Perovskite Thin Films with Moisture-Tolerant Molecules. *Nature Energy* **2016**, *1*, 15016.

(20) Zheng, X.; Chen, B.; Dai, J.; Fang, Y.; Bai, Y.; Lin, Y.; Wei, H.; Zeng, Xiao C.; Huang, J. Defect Passivation in Hybrid Perovskite Solar Cells Using Quaternary Ammonium Halide Anions and Cations. *Nat. Energy* **2017**, *2*, 17102.

(21) Cao, D. H.; Stoumpos, C. C.; Farha, O. K.; Hupp, J. T.; Kanatzidis, M. G. 2D Homologous Perovskites as Light-Absorbing Materials for Solar Cell Applications. *J. Am. Chem. Soc.* **2015**, *137*, 7843−7850.

(22) Quan, L. N.; Yuan, M.; Comin, R.; Voznyy, O.; Beauregard, E. M.; Hoogland, S.; Buin, A.; Kirmani, A. R.; Zhao, K.; Amassian, A.; Kim, D. H.; Sargent, E. H. Ligand-Stabilized Reduced-Dimensionality Perovskites. *J. Am. Chem. Soc.* **2016**, *138*, 2649−2655.

(23) Smith, I. C.; Hoke, E. T.; Solis-Ibarra, D.; McGehee, M. D.; Karunadasa, H. I. A Layered Hybrid Perovskite Solar-Cell Absorber with Enhanced Moisture Stability. *Angew. Chem., Int. Ed.* **2014**, *53*, 11232−11235.

(24) Zuo, C.; Scully, A. D.; Vak, D.; Tan, W.; Jiao, X.; McNeill, C. R.; Angmo, D.; Ding, L.; Gao, M. Self-Assembled 2D Perovskite Layers for Efficient Printable Solar Cells. *Adv. Energy Mater.* **2019**, *9*, 1803258.

(25) Liu, B.; Long, M.; Cai, M.; Ding, L.; Yang, J. Interfacial Charge Behavior Modulation in 2D/3D Perovskite Heterostructure for Potential High-Performance Solar Cells. *Nano Energy* **2019**, *59*, 715−720.

(26) Stoumpos, C. C.; Cao, D. H.; Clark, D. J.; Young, J.; Rondinelli, J. M.; Jang, J. I.; Hupp, J. T.; Kanatzidis, M. G. Ruddlesden−Popper Hybrid Lead Iodide Perovskite 2D Homologous Semiconductors. *Chem. Mater.* **2016**, *28*, 2852−2867.

(27) Hu, J.; Yan, L.; You, W. Two-Dimensional Organic−Inorganic Hybrid Perovskites: A New Platform for Optoelectronic Applications. *Adv. Mater.* **2018**, *30*, 1802041.

(28) Wang, Z.; Lin, Q.; Chmiel, F. P.; Sakai, N.; Herz, L. M.; Snaith, H. J. Efficient Ambient-Air-Stable Solar Cells with 2D−3D Heterostructured Butylammonium-Caesium-Formamidinium Lead Halide Perovskites. *Nat. Energy* **2017**, *2*, 17135.

(29) Tsai, H.; Nie, W.; Blancon, J.-C.; Stoumpos, C. C.; Asadpour, R.; Harutyunyan, B.; Neukirch, A. J.; Verduzco, R.; Crochet, J. J.; Tretiak, S.; Pedesseau, L.; Even, J.; Alam, M. A.; Gupta, G.; Lou, J.; Ajayan, P. M.; Bedzyk, M. J.; Kanatzidis, M. G.; Mohite, A. D. High-efficiency Two-Dimensional Ruddlesden−Popper Perovskite Solar Cells. *Nature* **2016**, *536*, 312−314.

(30) Zhang, X.; Ren, X.; Liu, B.; Munir, R.; Zhu, X.; Yang, D.; Li, J.; Liu, Y.; Smilgies, D.-M.; Li, R.; Yang, Z.; Niu, T.; Wang, X.; Amassian, A.; Zhao, K.; Liu, S. Stable High Efficiency Two-Dimensional

DOI: 10.1021/acsmaterialslett.9b00102
ACS Materials Lett. 2019, 1, 171−176

Perovskite Solar Cells via Cesium Doping. *Energy Environ. Sci.* **2017**, *10*, 2095−2102.
(31) Zhou, N.; Shen, Y.; Li, L.; Tan, S.; Liu, N.; Zheng, G.; Chen, Q.; Zhou, H. Exploration of Crystallization Kinetics in Quasi Two-Dimensional Perovskite and High Performance Solar Cells. *J. Am. Chem. Soc.* **2018**, *140*, 459−465.
(32) Zhang, X.; Wu, G.; Fu, W.; Qin, M.; Yang, W.; Yan, J.; Zhang, Z.; Lu, X.; Chen, H. Orientation Regulation of Phenylethylammonium Cation Based 2D Perovskite Solar Cell with Efficiency Higher Than 11%. *Adv. Energy Mater.* **2018**, *8*, 1702498.
(33) Lai, H.; Kan, B.; Liu, T.; Zheng, N.; Xie, Z.; Zhou, T.; Wan, X.; Zhang, X.; Liu, Y.; Chen, Y. Two-Dimensional Ruddlesden−Popper Perovskite with Nanorod-like Morphology for Solar Cells with Efficiency Exceeding 15%. *J. Am. Chem. Soc.* **2018**, *140*, 11639−11646.
(34) Yang, R.; Li, R.; Cao, Y.; Wei, Y.; Miao, Y.; Tan, W. L.; Jiao, X.; Chen, H.; Zhang, L.; Chen, Q.; Zhang, H.; Zou, W.; Wang, Y.; Yang, M.; Yi, C.; Wang, N.; Gao, F.; McNeill, C. R.; Qin, T.; Wang, J.; Huang, W. Oriented Quasi-2D Perovskites for High Performance Optoelectronic Devices. *Adv. Mater.* **2018**, *30*, 1804771.
(35) Ma, C.; Shen, D.; Ng, T.-W.; Lo, M.-F.; Lee, C.-S. 2D Perovskites with Short Interlayer Distance for High-Performance Solar Cell Application. *Adv. Mater.* **2018**, *30*, 1800710.
(36) Ke, W.; Mao, L.; Stoumpos, C. C.; Hoffman, J.; Spanopoulos, I.; Mohite, A. D.; Kanatzidis, M. G. Compositional and Solvent Engineering in Dion−Jacobson 2D Perovskites Boosts Solar Cell Efficiency and Stability. *Adv. Energy Mater.* **2019**, *9*, 1803384.
(37) Li, X.; Hoffman, J.; Ke, W.; Chen, M.; Tsai, H.; Nie, W.; Mohite, A. D.; Kepenekian, M.; Katan, C.; Even, J.; Wasielewski, M. R.; Stoumpos, C. C.; Kanatzidis, M. G. Two-Dimensional Halide Perovskites Incorporating Straight Chain Symmetric Diammonium Ions, $(NH_3C_mH_{2m}NH_3)(CH_3NH_3)_{n-1}Pb_nI3_{n+1}$ (m = 4−9; n = 1−4). *J. Am. Chem. Soc.* **2018**, *140*, 12226−12238.
(38) Li, Y.; Milić, J. V.; Ummadisingu, A.; Seo, J.-Y.; Im, J.-H.; Kim, H.-S.; Liu, Y.; Dar, M. I.; Zakeeruddin, S. M.; Wang, P.; Hagfeldt, A.; Grätzel, M. Bifunctional Organic Spacers for Formamidinium-Based Hybrid Dion−Jacobson Two-Dimensional Perovskite Solar Cells. *Nano Lett.* **2019**, *19*, 150−157.
(39) Ahmad, S.; Fu, P.; Yu, S.; Yang, Q.; Liu, X.; Wang, X.; Wang, X.; Guo, X.; Li, C. Dion-Jacobson Phase 2D Layered Perovskites for Solar Cells with Ultrahigh Stability. *Joule* **2019**, *3*, 794−806.
(40) Cohen, B.-E.; Li, Y.; Meng, Q.; Etgar, L. Dion−Jacobson Two-Dimensional Perovskite Solar Cells Based on Benzene Dimethanammonium Cation. *Nano Lett.* **2019**, *19*, 2588−2597.
(41) Patrick, C. R.; Prosser, G. S. A Molecular Complex of Benzene and Hexafluorobenzene. *Nature* **1960**, *187*, 1021.
(42) Coates, G. W.; Dunn, A. R.; Henling, L. M.; Dougherty, D. A.; Grubbs, R. H. Phenyl−Perfluorophenyl Stacking Interactions: A New Strategy for Supermolecule Construction. *Angew. Chem., Int. Ed. Engl.* **1997**, *36*, 248−251.
(43) Coates, G. W.; Dunn, A. R.; Henling, L. M.; Ziller, J. W.; Lobkovsky, E. B.; Grubbs, R. H. Phenyl−Perfluorophenyl Stacking Interactions: Topochemical [2+2] Photodimerization and Photopolymerization of Olefinic Compounds. *J. Am. Chem. Soc.* **1998**, *120*, 3641−3649.
(44) Dai, C.; Nguyen, P.; Marder, T. B.; Marder, T. B.; Scott, A. J.; Clegg, W.; Viney, C.; Viney, C. Control of Single Crystal Structure and Liquid Crystal Phase Behaviour via Arene−Perfluoroarene Interactions†. *Chem. Commun.* **1999**, 2493−2494.
(45) Ponzini, F.; Zagha, R.; Hardcastle, K.; Siegel, J. S. Phenyl/Pentafluorophenyl Interactions and the Generation of Ordered Mixed Crystals: sym-Triphenethynylbenzene and sym-Tris-(perfluorophenethynyl)benzene. *Angew. Chem., Int. Ed.* **2000**, *39*, 2323−2325.
(46) Feast, W. J.; Lövenich, P. W.; Puschmann, H.; Taliani, C. Synthesis and Structure of 4,4′-bis(2,3,4,5,6-pentafluorostyryl)stilbene, a Self-Assembling J Aggregate Based on Aryl−Fluoroaryl Interactions. *Chem. Commun.* **2001**, 505−506.
(47) Yan, L.; Hu, J.; Guo, Z.; Chen, H.; Toney, M. F.; Moran, A. M.; You, W. A General Post-Annealing Method Enables High-Efficiency Two-Dimensional Perovskite Solar Cells. *ACS Appl. Mater. Interfaces* **2018**, *10*, 33187−33197.
(48) Zhang, F.; Kim, D. H.; Lu, H.; Park, J.-S.; Larson, B. W.; Hu, J.; Gao, L.; Xiao, C.; Reid, O. G.; Chen, X.; Zhao, Q.; Ndione, P. F.; Berry, J. J.; You, W.; Walsh, A.; Beard, M. C.; Zhu, K. Enhanced Charge Transport in 2D Perovskites via Fluorination of Organic Cation. *J. Am. Chem. Soc.* **2019**, *141*, 5972−5979.
(49) Hu, J.; Oswald, I. W. H.; Stuard, S. J.; Nahid, M. M.; Zhou, N.; Williams, O. F.; Guo, Z.; Yan, L.; Hu, H.; Chen, Z.; Xiao, X.; Lin, Y.; Yang, Z.; Huang, J.; Moran, A. M.; Ade, H.; Neilson, J. R.; You, W. Synthetic Control over Orientational Degeneracy of Spacer Cations Enhances Solar Cell Efficiency in Two-Dimensional Perovskites. *Nat. Commun.* **2019**, *10*, 1276.
(50) Williams, O. F.; Guo, Z.; Hu, J.; Yan, L.; You, W.; Moran, A. M. Energy Transfer Mechanisms in Layered 2D Perovskites. *J. Chem. Phys.* **2018**, *148*, 134706.
(51) Liu, J.; Leng, J.; Wu, K.; Zhang, J.; Jin, S. Observation of Internal Photoinduced Electron and Hole Separation in Hybrid Two-Dimentional Perovskite Films. *J. Am. Chem. Soc.* **2017**, *139*, 1432−1435.
(52) Baker, J. L.; Jimison, L. H.; Mannsfeld, S.; Volkman, S.; Yin, S.; Subramanian, V.; Salleo, A.; Alivisatos, A. P.; Toney, M. F. Quantification of Thin Film Crystallographic Orientation Using X-ray Diffraction with an Area Detector. *Langmuir* **2010**, *26*, 9146−9151.
(53) Chen, A. Z.; Shiu, M.; Deng, X.; Mahmoud, M.; Zhang, D.; Foley, B. J.; Lee, S.-H.; Giri, G.; Choi, J. J. Understanding the Formation of Vertical Orientation in Two-dimensional Metal Halide Perovskite Thin Films. *Chem. Mater.* **2019**, *31*, 1336−1343.
(54) Chen, A. Z.; Shiu, M.; Ma, J. H.; Alpert, M. R.; Zhang, D.; Foley, B. J.; Smilgies, D.-M.; Lee, S.-H.; Choi, J. J. Origin of Vertical Orientation in Two-Dimensional Metal Halide Perovskites and its Effect on Photovoltaic Performance. *Nat. Commun.* **2018**, *9*, 1336.
(55) Zheng, H.; Liu, G.; Zhu, L.; Ye, J.; Zhang, X.; Alsaedi, A.; Hayat, T.; Pan, X.; Dai, S. The Effect of Hydrophobicity of Ammonium Salts on Stability of Quasi-2D Perovskite Materials in Moist Condition. *Adv. Energy Mater.* **2018**, *8*, 1800051.
(56) Xu, Z.; Mitzi, D. B. SnI_4^{2-}-Based Hybrid Perovskites Templated by Multiple Organic Cations: Combining Organic Functionalities through Noncovalent Interactions. *Chem. Mater.* **2003**, *15*, 3632−3637.
(57) Mitzi, D. B.; Medeiros, D. R.; Malenfant, P. R. L. Intercalated Organic−Inorganic Perovskites Stabilized by Fluoroaryl−Aryl Interactions. *Inorg. Chem.* **2002**, *41*, 2134−2145.
(58) Brown, N. M. D.; Swinton, F. L. The Importance of Quadrupolar Interactions in Determining the Structure of Solid Hydrocarbon−Fluorocarbon Compounds. *J. Chem. Soc., Chem. Commun.* **1974**, *0*, 770−771.
(59) Williams, J. H. The Molecular Electric Quadrupole Moment and Solid-State Architecture. *Acc. Chem. Res.* **1993**, *26*, 593−598.
(60) Du, K.-Z.; Tu, Q.; Zhang, X.; Han, Q.; Liu, J.; Zauscher, S.; Mitzi, D. B. Two-Dimensional Lead(II) Halide-Based Hybrid Perovskites Templated by Acene Alkylamines: Crystal Structures, Optical Properties, and Piezoelectricity. *Inorg. Chem.* **2017**, *56*, 9291−9302.
(61) Li, T.; Dunlap-Shohl, W. A.; Han, Q.; Mitzi, D. B. Melt Processing of Hybrid Organic−Inorganic Lead Iodide Layered Perovskites. *Chem. Mater.* **2017**, *29*, 6200−6204.
(62) Pollino, J. M.; Weck, M. Non-Covalent Side-Chain Polymers: Design Principles, Functionalization Strategies, And Perspectives. *Chem. Soc. Rev.* **2005**, *34*, 193−207.
(63) Biedermann, F.; Schneider, H.-J. Experimental Binding Energies in Supramolecular Complexes. *Chem. Rev.* **2016**, *116*, 5216−5300.
(64) Řezáč, J.; Hobza, P. Benchmark Calculations of Interaction Energies in Noncovalent Complexes and Their Applications. *Chem. Rev.* **2016**, *116*, 5038−5071.

DOI: 10.1021/acsmaterialslett.9b00102
ACS Materials Lett. 2019, 1, 171−176